Supplementary information: Field-controlled quantum anomalous Hall effect in electron-doped $CrSiTe_3$ monolayer: a first-principles prediction

Sungmo Kang[1], Seungjin Kang[1], Heung-Sik Kim[2,†], and Jaejun Yu[1,*]

[1]Center for Theoretical Physics, Department of Physics and Astronomy, Seoul National University, Seoul 08826, Korea
[2]Department of Physics and Institute of Quantum Convergence Technology, Kangwon National University, Chuncheon 24311, Korea
[*]jyu@snu.ac.kr
[†]heungsikim@kangwon.ac.kr

ABSTRACT

1 GRAPHIC OF MLWF AND SIMPLE TIGHT BINDING MODEL APPROACH

We first start with a graphene-like case for a simple tight-binding approach as a toy model. If we consider s band like orbital with NN hopping in a honeycomb lattice, the Dirac cone appears at the K point. When 2^{nd} and 3^{rd} NN hopping are taken into account, the Hamiltonian is given by following expressions which becomes more complicated

$$H(\mathbf{k}) = \begin{pmatrix} g(\mathbf{k}) & f(\mathbf{k}) \\ f^*(\mathbf{k}) & g(\mathbf{k}) \end{pmatrix}. \tag{1}$$

Component of above Hamiltonian $f(\mathbf{k})$ and $g(\mathbf{k})$ is written by

$$\begin{aligned} f(\mathbf{k}) &= t_1[e^{ik_y a/\sqrt{3}} + 2e^{-ik_y a/2\sqrt{3}} cos(k_x a/2)] \\ &\quad + t_3 e^{ik_y a/\sqrt{3}}(2cos(k_x a) + e^{-\sqrt{3}ik_y a}) \\ g(\mathbf{k}) &= t_2[2cos(k_x a) + 4cos(k_x a/2)cos(\sqrt{3}k_y a/2)], \end{aligned} \tag{2}$$

where $\mathbf{k} = (k_x, k_y)$, a is lattice constant and t_i is i^{th} NN hopping parameters. Diagonalizing the Hamiltonian expressed in Eq. 1,

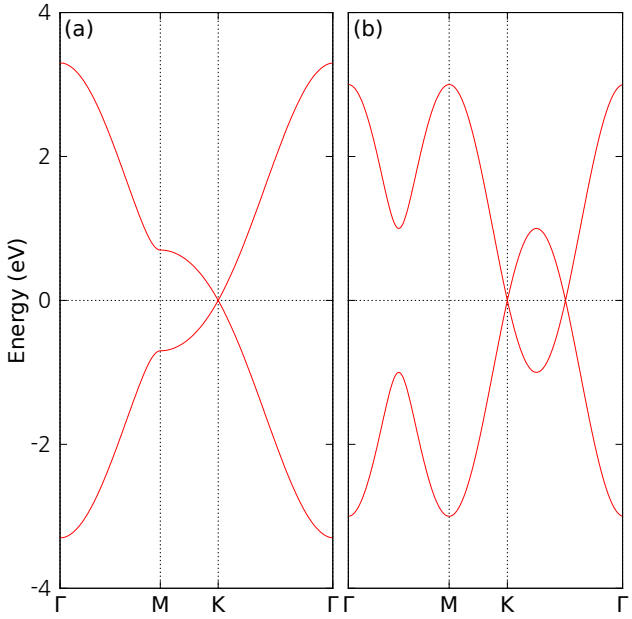

Figure 1. Band structure plot of simple s orbital like two band tight-binding model a Dominant 1^{st} NN hoping ($t_1 >> t_3$) and **b** dominant 3^{rd} NN hoping ($t_1 << t_3$) conditions. The 2^{nd} NN hopping term is set to be zero because it only affects energy shift of band diagram where overall features of band dispersion are remain unchanged.

one can obtain equation of eigenenergy function as follows.

$$\begin{aligned} E(\mathbf{k}) &= t_2(2cos(k_x a) + 4cos(k_x a/2)cos(\sqrt{3}k_y a/2)) \\ &\quad \pm [(t_1 + 2t_3 cos(k_x a)^2 + 2t_3 cos(\sqrt{3}k_y a)) + {t_3}^2 \\ &\quad + (t_1 + 2t_3 cos(k_x a))(4t_1 cos(k_x a/2)cos(\sqrt{3}k_y a/2) \\ &\quad + (2t_1 cos(k_x a/2))^2 + 4t_1 t_3 cos(k_x a/2)cos(\sqrt{3}k_y a/2)]^{1/2}. \end{aligned} \tag{3}$$

In this case, additional crossing point appears near the mid-point of Γ - K line under the condition of large 3^{rd} NN hopping parameter compared to 1^{st} and 2^{nd} NN hopping terms. This features are depicted in fig. 1.

(i, j)	${t^{(1)}}_{ij}$	${t^{(2)}}_{ij}$	${t^{(3)}}_{ij}$	${t^{(4)}}_{ij}$	${t^{(5)}}_{ij}$
$d_{x^2-y^2}, d_{x^2-y^2}$	-27.97	6.7	175.08	-2.42	36.94
$d_{x^2-y^2}, d_{z^2}$	2.55	14.46	10.21	1.76	0.64
$d_{z^2}, d_{x^2-y^2}$	1.51	13.7	3.65	1.77	1.09
d_{z^2}, d_{z^2}	-8.82	-18.03	-20.36	12.49	-14.85

Table 1. Hopping parameters based on converged MLWF basis. ${t^{(n)}}_{ij} = \langle$ i, 0 $|\hat{H}|$ j, $\vec{r_n}\rangle$, where i, j index indicates pair of MLWFs and $\vec{r_n}$ is cell displacement vector which corresponds to n^{th} NN site. Unit of hopping parameters is meV.

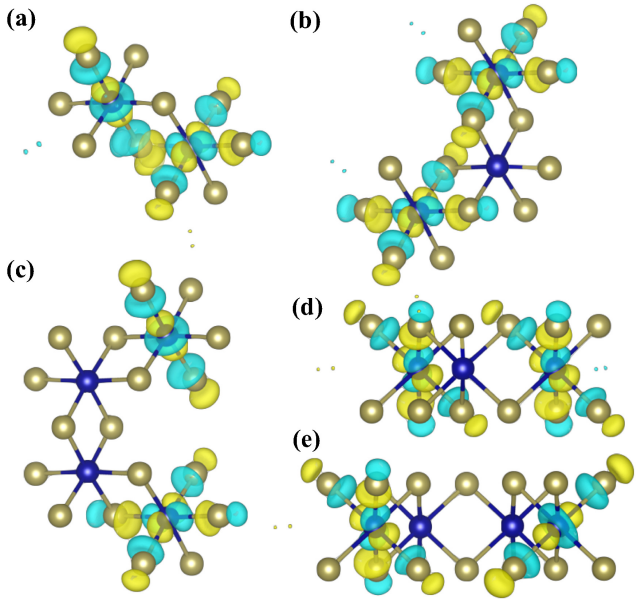

Figure 2. Graphic of converged MLWFs a top view of Nearest neighbor(NN), **b** 2^{nd} NN, **c** 3^{rd} NN and **d** side view of 2^{nd} NN, **e** 3^{rd} NN, respectively. MLWFs are constructed by combining four Cr e_g bands hybridized with Te p orbitals.

Table 1 shows the overlap matrix from our MLWF calculation result, which corresponds to hopping integrals in TB model analysis. One can find a significant 3^{rd} NN term compared to other terms which satisfy the condition of the above simple model approach. It can be confirmed qualitatively in Fig. 2 which shows converged MLWF graphically. Hopping between NN sites is small due to the orthogonality of mediating Te p orbitals. For 2^{nd} and 3^{rd} NN hopping, mediating two Te p orbitals are located in different layers for 2^{nd} NN case while in the same layer for 3^{rd} NN case, which induces much significant 3^{rd} NN hopping parameters compared to 1^{st} and 2^{nd} ones. This is a simple two-band model with s-like orbital to understand the shape of band structure briefly; thus, we considered a more realistic tight-binding model considering up to 5^{th} NN hopping with four band model in the tight-binding analysis part.

2 BANDGAP CLOSING DUE TO MIRROR SYMMETRY

If spin lies in-plane, its direction has chance to become vertical to one of three mirror planes of $CrSiTe_3$ which contain Γ - K line and perpendicular to its layer. When spin orientation is perpendicular to mirror plane, mirror symmetry would then be restored which is shown in Fig. 3. For case of $\phi = 90°$, 30° and 150°, band gap is closing near midpoint of Γ - K_n (where n=1,2,3) line, respectively while still maintaining at other points including K_n points. In Fig. 3(d), one can confirm each spin angle ($\phi = 30°, 90°, 150°$) corresponds to perpendicular to mirror plane (Γ - K_2, Γ - K_1, Γ - K_3), respectively. We may

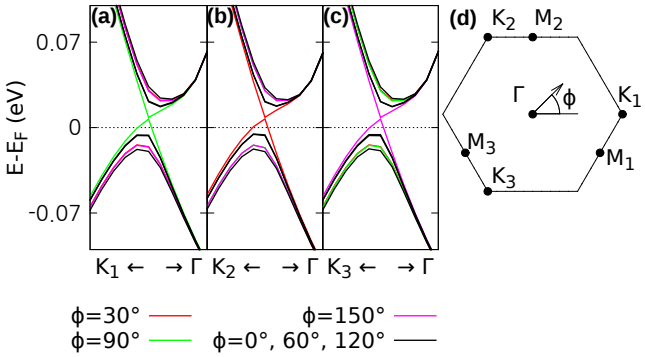

Figure 3. Band structure with spin easy plane ($\theta = 90°$) under two electron doping Expanded near middle of **a** Γ - K_1, **b** Γ - K_2 and **c** Γ - K_3 line, respectively. **d** First BZ with high symmetry points and in-plane spin angle ϕ.

conclude additional crossing points at Γ - K line originated from mirror symmetry of the system, while crossing at K point is from sublattice symmetry which is equivalent with graphene case.

3 Derivation of tight binding Hamiltonian

The full Hamiltonian H of on Cr-d and Te-p orbitals can be written as

$$H = H_0 + H_{CF} + H_{soc} + H_t + H_{\mathbf{B}_{\text{eff}}} \tag{4}$$

$$H_{CF} = \sum_{i,j=-2}^{2} V_{i,j}^{CF} d_i^{\dagger} d_j \tag{5}$$

$$H_{soc} = \lambda_p \hat{L_p} \cdot \hat{S}_p \tag{6}$$

$$H_0 = \sum_{\alpha,\mathbf{r}} \epsilon_d d_{\alpha,\mathbf{r}}^{\dagger} d_{\alpha,\mathbf{r}} + \sum_{\beta,\mathbf{r}} \epsilon_p p_{\beta,\mathbf{r}}^{\dagger} p_{\beta,\mathbf{r}} \tag{7}$$

$$H_t = \sum_{c,\alpha,\mathbf{r},\beta,\mathbf{r'}} V(\alpha,\mathbf{r},\beta,\mathbf{r'}) c_{\alpha,\mathbf{r}}^{\dagger} c_{\beta,\mathbf{r'}} \tag{8}$$

$$H_{\mathbf{B}_{\text{eff}}} = \sum_{\mathbf{r},\alpha,\tau,\tau'} [\mathbf{B}_{\text{eff}}(\mathbf{r}) \cdot \boldsymbol{\sigma}]_{\tau,\tau'} c_{\alpha,\tau,\mathbf{r}}^{\dagger} c_{\alpha,\tau',\mathbf{r}}, \tag{9}$$

where H_0, H_{CF}, H_{SOC}, H_t, and $H_{\mathbf{B}_{\text{eff}}}$ represent the orbital energy, crystal field on d orbitals, SOC, hopping, and effective Zeeman Hamiltonian, respectively. In the hopping Hamiltonian H_t, $V(\alpha,\mathbf{r},\beta,\mathbf{r'})$ represents the Slater-Koster parameter between orbital α at $\mathbf{r}$ and β at $\mathbf{r'}$. Since the magnitude of SOC on Te is much larger than Cr, we only include SOC Hamiltonian of p orbitals. The Zeeman Hamiltonian simulates the magneitc ordering. For instance, $\mathbf{B}_{\text{eff}}(\mathbf{r})$ is set to be the along [001] for all metal sites in the out-of-plane magnetization. This gives the magnetization-dependent hopping terms as Eq. 2 and Eq. 3 in our main article. To simplify the model, we integrate out the p orbital degree of freedom and construct the effective Hamiltonian on e_g orbitals through Kato-Takahashi perturbation formalism[1,2]. The explicit parameters are given as follow:

$$t_1 = V_{dd\pi}, \tag{10}$$

$$t_1^{'} = \frac{3V_{dd\pi}}{4} + \frac{V_{dd\sigma}}{4} \tag{11}$$

$$t_2 = \frac{V_{pd\sigma}^2 V_{pp\pi}}{(E_d - E_p)^2} \tag{12}$$

$$t_3 = \frac{V_{pd\sigma}^2(-V_{pp\pi} + V_{pp\sigma})}{4(E_d - E_p)^2} \tag{13}$$

$$t_5 = \frac{V_{pds}^2}{4(E_d - E_p)^3}(V_{ppp} - V_{pps})(V_{ddp} - V_{ppp} - V_{pps}) \tag{14}$$

$$t_{onsite}^{soc} = \frac{\sqrt{3}V_{pds}^2\lambda_p}{16(Ed - Ep)^3}(3V_{ddd} + 4V_{ddp} + V_{dds}) \tag{15}$$

$$t_1^{soc} = \frac{\sqrt{3}V_{pds}^2\lambda_p}{4(E_d - E_p)^2} \tag{16}$$

$$t_3^{soc} = \frac{\sqrt{3}V_{pds}^2\lambda_p(V_{ppp} + V_{pps})}{4(E_d - E_p)^3} \tag{17}$$

$$t_2^{soc} = \frac{\sqrt{3}V_{pds}^2\lambda_p(V_{ppp} - V_{pps})}{4(E_d - E_p)^3} \tag{18}$$

SUPPLEMENTARY REFERENCES

1. Kato, T. On the convergence of the perturbation method. i. *Prog. Theor. Exp. Phys.* **4**, 514–523, DOI: 10.1143/ptp/4.4.514 (1949).

2. Takahashi, M. Half-filled hubbard model at low temperature. *J. Phys. C: Solid State Phys.* **10**, 1289, DOI: 10.1088/0022-3719/10/8/031 (1977).